Study of the low temperature ordering of L10-Fe-Pt in Fe/Pt multilayers

Study of the low temperature ordering of L1$_0$–Fe–Pt in Fe/Pt multilayers

Yasushi Endo[a]
Department of Material Sciences and Engineering & Frontier Research Center,
Graduate School of Engineering, Osaka University, Yamada-Oka, Suita, Osaka 565-0871, Japan

Katsunari Oikawa
National Institute for Advanced Industrial Science and Technology, Nigatake 4-2-1, Miyagino-ku,
Sendai 983-8551, Japan

Takamichi Miyazaki, Osamu Kitakami, and Yutaka Shimada
Institute of Multidisciplinary Research for Advanced Materials, Tohoku University, Katahira 2-1-1, Aoba-ku,
Sendai 980-8577, Japan

In order to clarify the formation process of $L1_0$ Fe–Pt ordered phase in Fe (t_{Fe})/Pt (t_{Pt}) multilayers, we have evaluated the activation energy of ordering (Q_S) and of atomic interdiffusion at Fe/Pt interfaces (Q_D). Q_S for the multilayers takes a minimum value of ~0.7 eV when $t_{Fe} = t_{Pt}$, much lower than that of Fe–Pt disordered alloy films (1.2 eV). This value is almost the same with the activation energy Q_D of atomic interdiffusion at Fe/Pt interfaces. From these results, it is concluded that the interdiffusion at Fe/Pt interfaces which occurs at relatively low temperature dominates the formation process of $L1_0$ Fe–Pt in Fe/Pt multilayers. © *2003 American Institute of Physics.*
[DOI: 10.1063/1.1622997]

I. INTRODUCTION

For further improvement of ultrahigh-density magnetic recording media, a smaller grain size and isolation of ferromagnetic particles are essential. However, these requirements conflict with the thermal stability of the media. Recently, thin films composed of $L1_0$ Fe–Pt particles have been reported.[1,2] Thermal fluctuation of the particles is expected to be suppressed by their very large magnetocrystalline anisotropy of $10^7 - 10^8$ erg/cc.[3,4] However, high temperature treatment above 773 K is necessary for the formation of $L1_0$ ordered phase,[5–9] and this treatment is contradictory to the stability of the particulate structure. There have been a few reports concerning reduction of the ordering temperature.[10–15] We reported that some additives, such as Sn, Pb, Sb, Bi, and B, were effective in reducing the ordering temperature of Co–Pt.[10,11] The ordering temperature is significantly reduced by B which is interstitially incorporated along the c axis of $L1_0$ ordered phase. On the other hand, it has been reported that $L1_0$ Co– and Fe–Pt phases are formed in Co/Pt and Fe/Pt multilayers after annealing at very low temperatures.[12–15] We reported that, when the Fe and Pt layer thicknesses are exactly equal to each other, the multilayer structure disappears after annealing at 573 K and then the coercivity (H_c) tends to increase significantly,[14,15] but the reason why the formation of $L1_0$ ordered phases is promoted in the multilayers was not given explicitly in previous work. Artymowicz *et al.* reported that the activation energy of ordering evaluated from the time dependence of the PtCo(001) intensity in their multilayers is as low as 2.1 eV, significantly lower than that of self-diffusion of Co and Pt.[12] They suggested that the reason for this lower energy is gradient-assisted diffusion due to the multilayer structure and also the large chemical diffusivity of Co in Pt.

In this article, we determine the degree of ordering (S^2) of Fe/Pt multilayers annealed at various temperatures, and evaluate the activation energy of ordering (Q_S). Furthermore, we experimentally evaluate the activation energy of interdiffusion at Fe/Pt interfaces (Q_D) and clarify the relationship between these two activation energies.

II. EXPERIMENTAL PROCEDURE

Multilayers of Fe/Pt were deposited on fused quartz substrates at ambient temperature in a dc magnetron sputtering system. The base pressure of the sputtering system was less than 8.0×10^{-5} Pa and the Ar gas pressure during deposition was maintained at 0.4 Pa. Layers of Fe and Pt were deposited at a rate of 0.10–0.12 nm/s and 0.09–0.11 nm/s, respectively. The Fe layer thickness was fixed at $t_{Fe} = 2.5$ nm while the Pt layer thickness t_{Pt} was varied from 0.5 to 5.0 nm. For all the multilayers studied in this article, the number of Fe and Pt layers was fixed at 10. Annealing was performed at temperatures of 473–773 K in vacuum lower than 1.3×10^{-4} Pa. In addition, 100 nm thick FePt single layers were fabricated and annealed under the same conditions. Details of the sputtering conditions are given in Ref. 16. The lattice constants (a and c axes) and the degree of ordering (S^2) were determined by x-ray diffraction (XRD) with Cu $K\alpha$ radiation. The film compositions in Fe/Pt multilayers were confirmed by electron probe microanalysis (EPMA) and XRD. The thicknesses of Fe and Pt layers were determined accurately by numerical fitting to the small-angle XRD patterns and the composition was confirmed from the thickness ratio of each layer. The room temperature magnetic properties were measured with a

[a]Author to whom correspondence should be addressed; electronic mail: endo@mat.eng.osaka-u.ac.jp

vibrating sample magnetometer in a maximum field of 1.2 $\times 10^3$ kA/m. Bilayers of Fe (100 nm)/Pt (100 nm) were prepared specifically under the exact same sputtering conditions as those described in Ref. 16 to evaluate the activation energy (Q_D) of interdiffusion at the Fe/Pt interface. In this case, annealing was carried out at 523–673 K for 1 min; and then these samples were quenched in water. Interdiffusion at the interface of the Fe/Pt bilayers were determined by Auger electron spectroscopy (AES) from which the diffusion constant (D) and Q_D were evaluated.

III. RESULTS AND DISCUSSION

The degree of ordering S is defined as[17]

$$S = 2(\gamma_\alpha - x_{\text{Fe}}) = 2(\gamma_\beta - x_{\text{Pt}}), \tag{1}$$

where sites α and β are for Fe atoms and Pt atoms in the fully ordered $L1_0$ structure, and γ_α and γ_β are the fraction of α and β sites occupied by the right atom, and x_{Fe} and x_{Pt} are the atomic fractions of Fe and Pt, respectively. $S = 1$ means that the phase is fully ordered when the composition is stoichiometric with $\gamma_\alpha = \gamma_\beta = 1$. Deviation of the composition from 0.5 (deviation of either γ_α or γ_β from 1) results in $S < 1$. For the sample with nominal layer thickness of 2.5 nm for both Fe and Pt, the composition was determined to be Fe:Pt$=0.52:0.48$ by EPMA.[14] This is very close to 0.5:0.5 and S is evaluated as 0.94 by Eq. (1) for the perfectly ordered $L1_0$. Another way to evaluate S is accurate determination of the lattice parameters by XRD. The degree of ordering (S^2) is given by[18]

$$S^2 = \frac{1 - c/a}{1 - (c/a)_{\text{eq}}}, \tag{2}$$

where $(c/a)_{\text{eq}}$ is the fully ordered lattice and is 0.96 for our samples. The accuracy of the ratio (c/a) can be improved appreciably by the Cohen method.[19] It is well known that the systematic error for Bragg angle θ can be described well by the Nelson–Riley function.[20] The Bragg condition for a tetragonal lattice can be expressed with this function as

$$\sin^2 \theta = A(h^2 + k^2) + Bl^2 + C\left\{ 10 \sin^2 2\theta \left(\frac{1}{\sin \theta} + \frac{1}{\theta} \right) \right\}, \tag{3}$$

where A, B, and C are $\lambda^2/4a^2$, $\lambda^2/4c^2$, and a constant, respectively, and λ is the x-ray wavelength. The accuracy of this method was already confirmed in Ref. 21. The θ–2θ scans for the samples shown in Fig. 1(a) indicates that (111) planes are preferably grown and the superstructure peaks cannot be identified. As shown in Fig. 1(b), the glancing angle incident of the x-ray beam made it possible to observe them and to determine coefficients A, B, and C by least-square fitting. The results are shown in Fig. 2. All data points determined by Eq. (3) are exactly on a single straight line. Thus lattice constants determined are $a=0.3844 \pm 0.0002$ nm, $c=0.3765 \pm 0.0005$ nm for $T_a = 623$ K, and $a = 0.3866 \pm 0.0001$ nm, $c=0.3713 \pm 0.0002$ nm for $T_a = 773$ K. From these results, we can clarify variation of the lattice constants of $L1_0$ Fe–Pt phase in Fe/Pt multilayers in the annealing process at $T_a \gtrsim \sim 550$ K within an error of
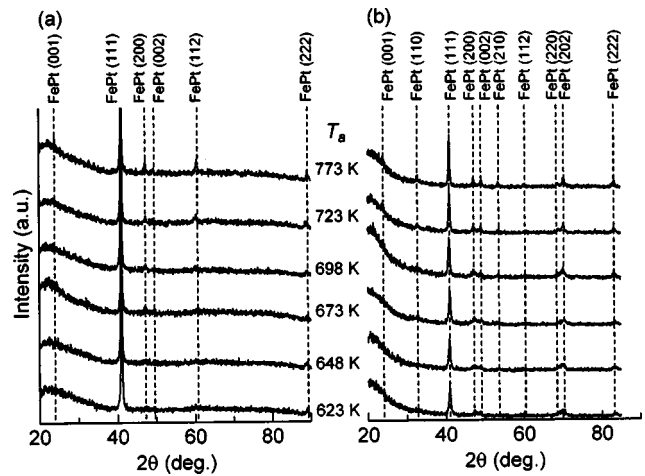

FIG. 1. X-ray diffraction patterns for $[\text{Fe}(2.5 \text{ nm})/\text{Pt}(2.5 \text{ nm})]_{10}$ multilayers at various annealing temperatures (T_a): (a) high angle; (b): glancing angle 2θ scan.

0.2%. Figure 3 shows the annealing temperature dependence of the axial ratio (c/a) for Fe (2.5 nm)/Pt (t_{Pt}) multilayers where $t_{\text{Pt}}=1.5$, 2.5, and 3.5 nm. Note that c/a decreases rapidly with T_a up to 698 K and then tends to become constant. It is obvious that the ratio of c/a for Fe/Pt multilayers saturates at lower annealing temperatures than that for the single layer FePt film. Here, we assume that c/a for $T_a = 773$ K is $(c/a)_{\text{eq}}$ for the multilayers and that for T_a

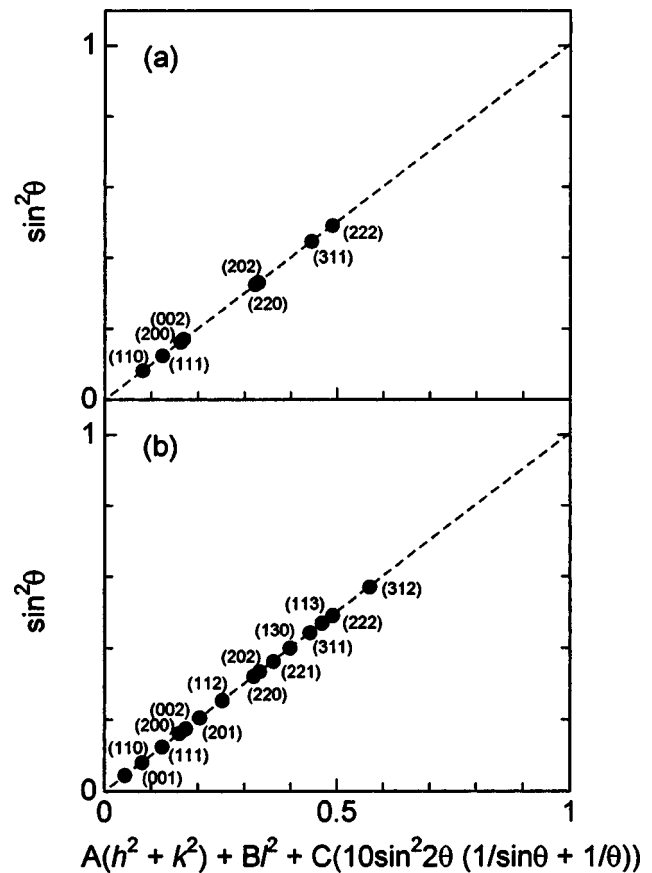
FIG. 2. Examples of determination of lattice constants for $L1_0$ Fe–Pt phase in Fe/Pt multilayers using Cohen's method. $T_a=$ (a) 623 and (b) 773 K.
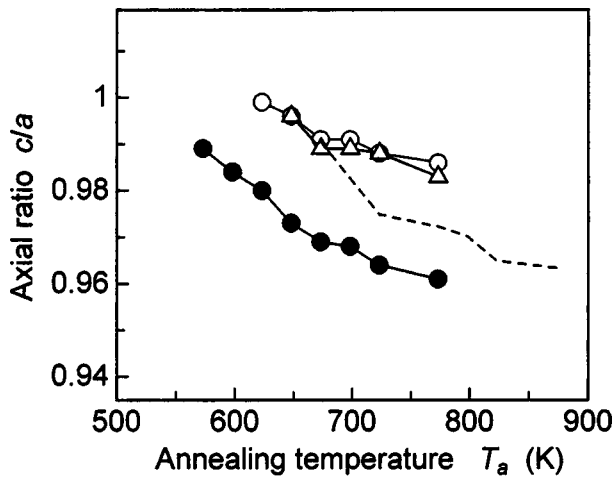
FIG. 3. Annealing temperature (T_a) dependence of the ratio (c/a) for $[\text{Fe}(2.5\ \text{nm})/\text{Pt}(t_{\text{Pt}})]_{10}$ ($t_{\text{Pt}}=1.5$, 2.5, and 3.5 nm) multilayers. ($\bigcirc$), ($\bullet$), ($\triangle$): $t_{\text{Pt}}=1.5$, 2.5, and 3.5 nm, respectively. The broken line represents a 100 nm thick FePt film.

$=873$ K is $(c/a)_{\text{eq}}$ for the single layer sample, and by substituting these values in Eq. (2), S^2 was determined. The results are shown in Fig. 4. The behavior of S^2 is obviously analogous to that of H_c. In particular, for $t_{\text{Pt}}=2.5$ nm (closed circle in Fig. 4), ordering has already started by annealing at temperature as low as 573 K, and obviously this is the fastest among three samples.

If the composition is nonstoichiometric and $S\neq0$, the relationship between Q_S and S^2 is expressed as follows:[22]

$$\frac{v_1}{v_2}\exp\left(-\frac{Q_S S}{k_B T}\right)=\frac{\gamma_i(1-\gamma_i)-\frac{1}{2}S+\frac{1}{4}S^2}{\gamma_i(1-\gamma_i)+\frac{1}{2}S+\frac{1}{4}S^2},\tag{4}$$

where v_i ($i=1,2$) is the arbitrary parameter, $\gamma_i(i=\alpha,\beta)$ is the fraction of i sites occupied by the A (or B) atom, and k_B and T are the Boltzmann constant and the temperature, respectively. By rewriting Eq. (4),

FIG. 5. Relationship between y and x for the postannealed $[\text{Fe}(2.5\ \text{nm})/\text{Pt}(2.5\ \text{nm})]_{10}$ multilayers.

$$y=A-\left(\frac{Q_S}{k_B}\right)x,\tag{5}$$

where

$$A=\ln\left(\frac{v_1}{v_2}\right),$$

$$x=\left(\frac{S}{T}\right),$$

and

$$y=\ln\left(\frac{\gamma_i(1-\gamma_i)-\frac{1}{2}S+\frac{1}{4}S^2}{\gamma_i(1-\gamma_i)+\frac{1}{2}S+\frac{1}{4}S^2}\right),$$

respectively.

In Fig. 5, y is plotted versus x. By least-square fitting, Q_S is evaluated to be 0.7 eV from Eq. (5). Figure 6 shows the activation energy for Q_S as a function of the thickness ratio $t_{\text{Pt}}/t_{\text{Fe}}$ with Q_S of a 100 nm thick FePt film as a reference.
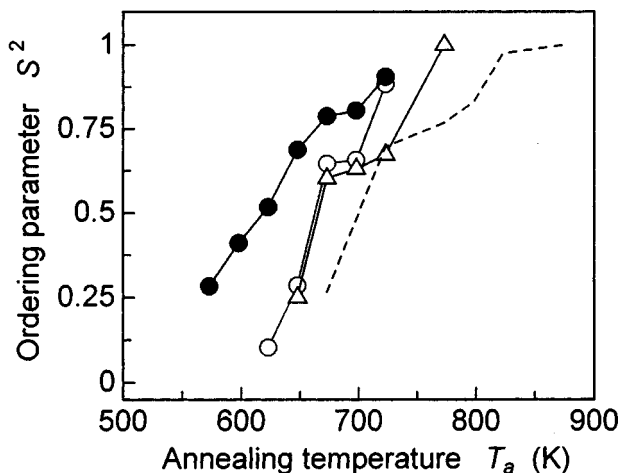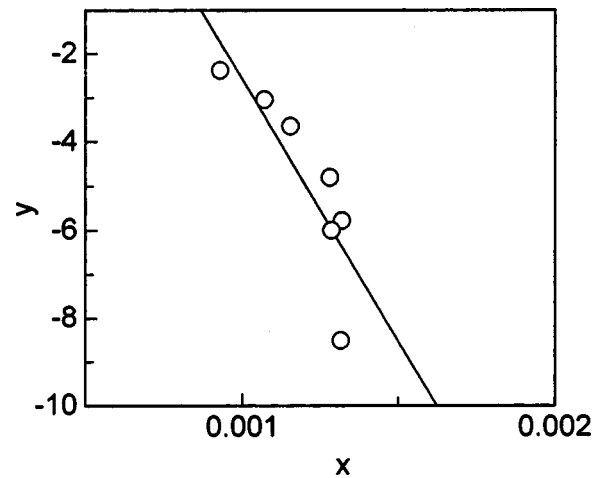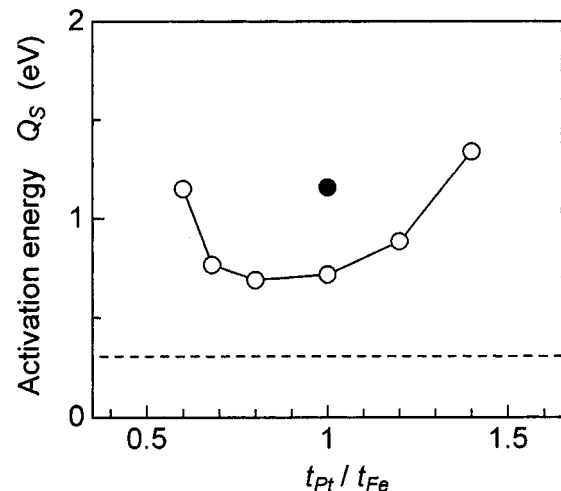

FIG. 4. Ordering parameter (S^2) for $[\text{Fe}(2.5\ \text{nm})/\text{Pt}(t_{\text{Pt}})]_{10}$ ($t_{\text{Pt}}=1.5$, 2.5, and 3.5 nm) multilayers as a function of the annealing temperature (T_a). ($\bigcirc$), ($\bullet$), ($\triangle$): $t_{\text{Pt}}=1.5$, 2.5, and 3.5 nm, respectively. The broken line represents a 100 nm thick FePt film.

FIG. 6. Activation energy of ordering (Q_S) as a function of the thickness ratio ($t_{\text{Pt}}/t_{\text{Fe}}$). ($\bullet$): 100 nm thick FePt films. The broken line is the activation energy of interdiffusion (Q_D).
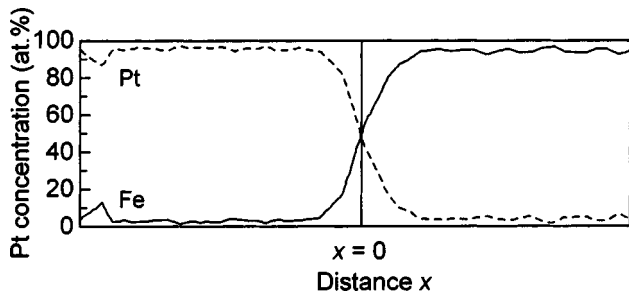
FIG. 7. Depth profile of the Fe(100 nm)/Pt(100 nm) bilayer for T_a = 623 K.

For the samples with $t_{Pt}/t_{Fe} < 0.7$ and $t_{Pt}/t_{Fe} > 1.2$, Q_S is over 1.0 eV while for $0.7 \leq t_{Pt}/t_{Fe} \leq 1.2$, Q_S takes a minimum value of 0.70 eV. This value is much smaller than that of the 100 nm thick FePt film, and is also significantly lower than that for self-diffusion energy of Fe (1.73 eV) and Pt (2.89 eV).[23] So we conclude that the ordering process of Fe/Pt multilayers which begins at lower annealing temperature is because of the smaller activation energy (Q_S) in Fe/Pt multilayers with equal thicknesses of Fe and Pt.

In order to clarify the origin of the small activation energy, we evaluated the diffusion constants of Fe and Pt at Fe/Pt interfaces using Fe (100 nm)/Pt (100 nm) diffusion couples. After rapid annealing at $T = 523, 573, 623,$ and 673 K for 60 s, we measured the compositional depth profiles at the interfaces by Auger electron spectroscopy. A representative profile of the diffusion couple annealed at $T = 623$ K is shown in Fig. 7. By analyzing these depth profiles in accordance with well-known Matano analysis,[24] we determined the compositional dependence of the diffusion constants for all the samples at various temperatures. These results are given in Fig. 8. From these relations, $\ln D$ for Pt concentration of 50 at. % were plotted against the inverse of the annealing temperature ($1/T_a$), shown in Fig. 9. Since the dif-
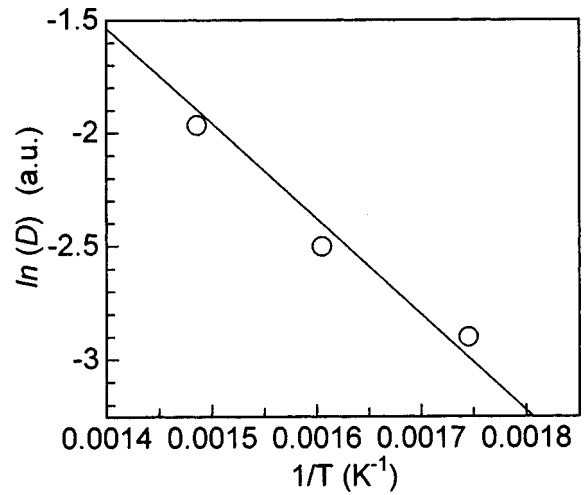
FIG. 9. Relationship between $\ln D$ and $1/T$ for a Pt concentration of 50 at. %.

fusion constant D is expressed as $D = D_0 \exp(-Q_D/k_B T)$, where D_0 and Q_D are a constant and the activation energy for the diffusion, respectively, Q_D is determined to be 0.31 eV from the slope in Fig. 9. The Q_D determined is depicted in Fig. 6 by the broken line in comparison with Q_S for the multilayers. The multilayers have higher Q_S than Q_D. The reason is that Q_S includes the process of crystal phase transformation from face centered cubic (fcc) to face centered tetragonal (fct) as ordering proceeds.

Moreover, from the results of structural analyses and magnetic measurements, the absolute value of the thickness of each layer should also be considered as the important parameter for low temperature ordering of Fe–Pt in Fe/Pt multilayers. Ordering starts at temperatures as low as 573 K when the absolute value of the thickness of each layer is almost equal and is in the range of 1.5–2.5 nm. This optimum thickness range suggests a strong correlation between the multilayer dimensions and the speed of interdiffusion and it is an important subject to study in the future.

IV. CONCLUSION

In order to clarify the ordering process of $L1_0$ Fe–Pt phase in Fe/Pt multilayers, we have evaluated the activation energy of ordering (Q_S) and of interdiffusion at the Fe/Pt interface (Q_D). The activation energy Q_S takes a minimum of ~0.70 eV when the Fe and Pt layer thicknesses are equal. This value is much smaller than that of the Fe–Pt single layer (1.15 eV), and also lower than the self-diffusion energy for Fe (1.73 eV) and Pt (2.89 eV). It turned out that this value is close to the activation energy of interdiffusion at the Fe/Pt interface (Q_D). Therefore, it is concluded that the enhanced ordering process of the multilayers is directly correlated with the rapid interdiffusion at the Fe/Pt interface.
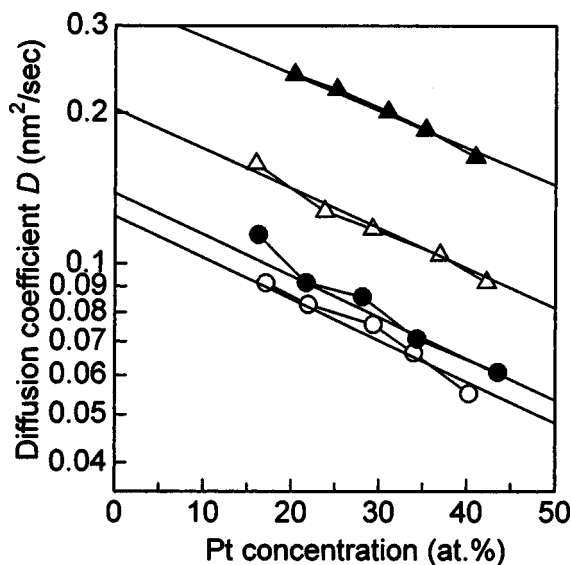
FIG. 8. Diffusion constants determined by AES as a function of the Pt concentration. (○), (●), (△), (▲): $T_a = 523, 583, 623,$ and 673 K, respectively.

performing the AES depth profile. The 2θ scan XRD measurements were performed at the Laboratory for Development Research of Advanced Materials, Institute for Material Research, Tohoku University. This work was supported by the Society for the Promotion of Science under Grant No. 97R14701, the Research for the Future Program of Japan, and the Storage Research Consortium of Japan.

[1] K. R. Coffey, M. A. Parker, and J. K. Howard, IEEE Trans. Magn. **31**, 2737 (1973).
[2] S. Sun, C. B. Murray, D. Weller, L. Folks, and A. Moser, Science **287**, 1989 (2000).
[3] R. A. McCurrie and P. Gaunt, Philos. Mag. **13**, 567 (1966).
[4] V. V. Maykov, A. Ye. Yermakov, G. V. Ivanov, V. I. Khrabrov, and L. M. Magat, Phys. Met. Metallogr. **67**, 76 (1989); **69**, 198 (1990).
[5] M. R. Visokay and R. Sinclair, Appl. Phys. Lett. **66**, 1692 (1995).
[6] S. Stavroyiannis, I. Panagiotopoulos, D. Niarchos, J. A. Chistodoulides, Y. Yang, and G. C. Hadjipanayis, Appl. Phys. Lett. **73**, 3453 (1998).
[7] A. Cebollada, D. Weller, J. Sticht, G. R. Harp, R. F. C. Farrow, R. Marks, R. Savoy, and J. C. Scott, Phys. Rev. B **50**, 3419 (1994).
[8] V. Parasote, M. C. Cadeville, G. Garreau, and E. Beaurepaire, J. Magn. Magn. Mater. **198–199**, 375 (1999).
[9] R. F. C. Farrow, D. Weller, R. F. Marks, M. F. Toney, S. Hom, G. R. Harp, and A. Cebollada, Appl. Phys. Lett. **69**, 1166 (1996).
[10] O. Kitakami, Y. Shimada, K. Oikawa, H. Daimon, and K. Fukamichi, Appl. Phys. Lett. **78**, 1104 (2001).
[11] H. Yamaguchi, O. Kitakami, S. Okamoto, Y. Shimada, K. Oikawa, and K. Fukamichi, Appl. Phys. Lett. **79**, 2001 (2001).
[12] D. M. Artymowicz, B. M. Lairson, and B. M. Clemens, J. Cryst. Growth **169**, 83 (1996).
[13] C. P. Luo and D. J. Sellmyer, IEEE Trans. Magn. **31**, 2764 (1995).
[14] Y. Endo, N. Kikuchi, O. Kitakami, and Y. Shimada, J. Magn. Soc. Jpn. **25**, 835 (2001).
[15] Y. Endo, N. Kikuchi, O. Kitakami, and Y. Shimada, J. Appl. Phys. **89**, 7065 (2001).
[16] H. Sakaue, T. Miyazaki, O. Kitakami, and Y. Shimada, J. Magn. Soc. Jpn. **25**, 847 (2001).
[17] B. E. Warren, *X-ray Diffraction* (Dover, New York, 1990) pp. 208–210.
[18] B. W. Roberts, Acta Metall. **2**, 597 (1954).
[19] M. U. Cohen, Rev. Sci. Instrum. **6**, 68 (1935); **7**, 155 (1936).
[20] J. B. Nelson and D. P. Riley, Proc. R. Soc. London **57**, 126 (1945).
[21] S. Okamoto, O. Kitakami, and Y. Shimada, J. Magn. Magn. Mater. **208**, 102 (2000).
[22] G. J. Dienes, Acta Metall. **3**, 549 (1955).
[23] http://www.dfw.jst.go.jp/difdb
[24] C. Matano, Jpn. J. Phys. **8**, 109 (1933).